BJA

British Journal of Anaesthesia, 123 (3): 298–308 (2019)

doi: 10.1016/j.bja.2019.05.038
Advance Access Publication Date: 2 July 2019
Neuroscience and Neuroanaesthesia

NEUROSCIENCE AND NEUROANAESTHESIA

Transient subcortical functional connectivity upon emergence from propofol sedation in human male volunteers: evidence for active emergence

Tommer Nir[1,*,†], Ayelet Or-Borichev[2,3,†], Evgeny Izraitel[1], Talma Hendler[2,3,4], Yulia Lerner[2,3,5,‡] and Idit Matot[1,3,‡]

[1]Division of Anaesthesia, Intensive Care and Pain Medicine, Tel Aviv Medical Center, Tel Aviv, Israel, [2]Sagol Brain Institute, Tel Aviv Sourasky Medical Center, Tel Aviv, Israel, [3]Sackler Faculty of Medicine, Tel Aviv University, Tel Aviv, Israel, [4]School of Psychological Sciences, Tel Aviv University, Tel Aviv, Israel and [5]Sagol School of Neuroscience, Tel Aviv University, Tel Aviv, Israel

*Corresponding author. E-mail: Tommer.Nir@mountsinai.org

[†]These authors contributed equally to this work.
[‡]These authors contributed equally to this work.

This article is accompanied by an editorial: Finding the starter motor for the engine of consciousness by Sleigh & Warnaby, *Br J Anaesth* 2019:123:259–261, https://doi.org/10.1016/j.bja.2019.06.001.

Abstract

Background: Emergence from sedation entails rapid increase in the levels of both awareness and wakefulness, the two axes of consciousness. Functional MRI (fMRI) studies of emergence from sedation often focus on the recovery period, with no description of the moment of emergence. We hypothesised that by focusing on the moment of emergence, novel insights, primarily about subcortical activity and increased wakefulness, will be gained.

Methods: We conducted a resting state fMRI analysis of 17 male subjects (20–40 yr old) gradually entering into and emerging from deep sedation (average computed propofol concentrations of 2.41 and 1.11 μg ml^{-1}, respectively), using target-controlled infusion of propofol.

Results: Functional connectivity analysis revealed a robust spatiotemporal signature of return of consciousness, in which subcortical seeds showed transient positive correlations that rapidly turned negative shortly after emergence. Elements of this signature included four components of the ascending reticular activating system: the ventral tegmentum area, the locus coeruleus, median raphe, and the mammillary body. The involvement of the rostral dorsolateral pontine tegmentum, which is specifically impaired in comatose patients with pontine lesions, in emergence was previously unknown.

Conclusions: Emergence from propofol sedation is characterised, and possibly driven, by a transient activation of brainstem loci. Some of these loci are known components of the ascending reticular activating system, whereas an additional locus was found that is also impaired in comatose patients.

Keywords: ascending reticular activating system; brainstem; coma; consciousness; emergence; MRI; propofol; sedation

Editorial decision:16 May 2019; **Accepted:** 16 May 2019

Editor's key points

- The mechanisms underlying emergence from anaesthesia and sedation are important clinically and provide insights into the neurobiology of consciousness.
- The authors analysed resting-state fMRI analysis of brain activity during entry into and emergence from deep sedation by target-controlled infusion of propofol.
- Emergence from propofol sedation was characterised by transient activation of brainstem loci involved in the ascending reticular activating system.
- This observed functional connectivity spatiotemporal sequence suggests that emergence from sedation is an active subcortically driven process.

Emergence from sedation induced by hypnotic drugs is of clinical significance in human anaesthesia and a good model for studying dynamics of states of consciousness. Previous human studies[1–3] using EEG, positron emission tomography (PET), and functional MRI (fMRI) have advanced our understanding yet also demonstrated the methodological challenge in unveiling the emergence dynamics phenomena. One challenge is the timing of emergence. EEG temporal resolution allows for objective marking of the moment of emergence.[1] Yet, the critical involvement of brainstem loci that are poorly measured by scalp EEG recording precludes satisfactory investigation of the neural mechanisms that underlie regulation of wakefulness. To overcome this spatial resolution hurdle, modalities such as PET and fMRI could be used, albeit at the cost of low temporal resolution. Another challenge focuses on personalised aspects of emergence; individuals exhibit different emergence dynamics with respect to their pharmacological anaesthetic status. One way of dealing with this challenge is to use a common design of estimated 'sedation' *vs* 'recovery'—without an accurate probing of the individual moment of emergence. Another approach to overcome both the temporal and personalisation challenges is to reduce the variability of the moment of emergence. This could be done either via abrupt cessation of administered hypnotics[1,2] or administration of drugs to facilitate emergence (e.g. methylphenidate,[4] modafinil,[5] physostigmine,[3] and an orexin agonist[6]), either of which shorten and sharpen the lag between withdrawal of the hypnotic agent to eye opening, at the cost of the introduction of another factor to the already complex phenomenon of emergence.

We sought to overcome these challenges by coupling the use of resting state fMRI, which can resolve subcortical structures, with analysis of tightly clustered time windows before, during, and immediately after emergence from propofol deep sedation. We compared the resting state activity of the brain before and after the point of regaining response to verbal command to find which specific areas increased their activity significantly. Then we examined how the functional connectivity of these areas (regions of interest [ROIs]) with the rest of the brain changed during emergence.

We studied healthy adult male subjects, who while lying in the fMRI scanner were subjected to a gradually increasing level of sedation through controlled increments of propofol infusion. Subsequently, a similarly graded decrement of propofol led to emergence. This experimental approach minimised the effect of changing drug concentrations on emergence by allowing equilibration of drug levels in the brain at each level of increment/decrement.

Based on previous suggestions,[7,8] we hypothesised that emergence from sedation shares common features with other alterations of consciousness and arousal, including sleep and coma. Therefore, our fMRI analyses focused mainly on subcortical regions known to promote wakefulness and sleep–wake transitions: a group of nuclei in the ascending reticular activating system (ARAS) including the pons, through the midbrain and thalamus up to the basal forebrain. The ARAS has been studied extensively,[9,10] both in relation to sleep and anaesthesia, in animals and humans.[11,12] Another ROI not previously regarded as a component of the ARAS, but which has been identified as critical in comatose patients, is the rostral dorsolateral pontine tegmentum (RDLPT).[13,14] By focusing on these regions, we identified a robust signature of return of consciousness (ROC) that ties modulation of consciousness by hypnotic drugs to both sleep and coma.

Methods

Subjects

Twenty-five healthy male subjects (ages 20–40 yr, ASA physical status 1) from the local community with a dominant right hand provided informed consent for their participation in the study. Three participants were excluded because of medical conditions. Data from five subjects were excluded from the analyses because of excessive movement throughout the scan (see "Preprocessing" section below). Thus, data from 17 participants are presented. Procedures were approved by the Helsinki Committee on Activities Involving Human Subjects in the Tel Aviv Sourasky Medical Center (TASMC), Tel Aviv, Israel.

Sedation and monitoring

Subjects abstained from any medication for 24 h before the study session and fasted overnight. Participants were placed in the MRI scanner and continuously monitored Invivo Expression (Gainseville, FL. USA) for heart rate, SpO_2 and end-tidal CO_2. After baseline acquisition, sedation ensued by target-controlled infusion (TCI) of propofol Lipuro 20 mg ml^{-1} (Braun, Melsungen, Germany) with an Alaris PK (BD, San Diego, CA. USA) syringe pump, using a Schnider protocol. Propofol infusion was initially set to a plasma concentration of 1 μg ml^{-1} with 0.5 μg ml^{-1} increments every 5 min. Participants' responses were assessed every minute. After achieving a Modified Ramsay Scale[15] score of 5/6, no response to repeated loud verbal stimuli (an anaesthesiologist near the scanner calling their name), we determined loss of consciousness (LOC). Duration of this stage varied slightly between participants because of variable LOC entry points. Gradual 0.5 μg ml^{-1} decrements of propofol infusion were made every 5 min until subjects opened their eyes in response to a verbal stimulus (name + open your eyes), defined as ROC. Participants remained in the MRI scanner until fMRI acquisition ended. Subjects were monitored for another hour, and were discharged only after meeting appropriate criteria as per TASMC guidelines.

Experimental procedure

A preliminary interview, before the fMRI session, was conducted with each subject which included an explanation of the study and experimental procedures, pre-anaesthesia physical checkup, and signing of informed consent. On the day of the scan, subjects were placed in the scanner after verifying their

well-being in a brief conversation. Acquisition included two consecutive sequences. The first sequence (30 min) included a baseline without propofol, followed by gradual sedation with propofol TCI as described above until LOC was achieved. After a brief pause owing to safety concerns of overheating, the second sequence (36 min) followed and comprised 5 min of sedation before graded decrements of propofol led to ROC. A typical session lasted 75 min.

fMRI data acquisition

fMRI scanning was performed with a 3.0 T Signa Excite echo speed scanner (General Electric Medical Systems, Waukesha, WI. USA) using a 20-channel head coil at the TASMC. The MR protocol consisted of high-resolution FLASH T1-weighted imaging (T1WI), with field of view (FOV)=256 mm, matrix=256×256, slice thickness of 1 mm (1 mm iso voxel), and TR/TE=1860/2.74 ms. Functional whole-brain scans were performed in interleaved order with a T2*-weighted gradient echo planar imaging pulse sequence (TR/TE=2500/30 ms, flip angle=90°, FOV=220 mm, slice thickness=3 mm, 42 slices, 861 volumes). Optoactive II MRI-compatible headphones (Optoacoustics, Mazor, Israel) were used to attenuate the scanner noise and to communicate with subjects.

Preprocessing

BrainVoyagerQX version 2.8.4 (Brain Innovation, Maastricht, The Netherlands) was used for preprocessing and co-registration of standardised anatomical and functional data. Data analysis was performed separately for each subject. Data were high pass filtered at 0.002 Hz and spatially smoothed with a 4 mm full-width at half-maximum (FWHM) kernel. Head motions were detected and corrected using trilinear/sinc interpolation. Owing to extensive head movements (deviations higher than 2 mm), five subjects were excluded from the study. The cortical surface was reconstructed from the anatomical images using standard procedures implemented in the BrainVoyager software. The complete functional dataset was transformed to a common 3D Talairach space[16] and projected on a reconstruction of the cortical surface.

Selection of time windows

Subjects attained ROC and LOC at different propofol concentrations and therefore, at different time points throughout the resting state fMRI. By aligning all subjects' scans around the primary event, which was defined as emergence from deep sedation (ROC), we were able to conduct group analyses. Although continuous fMRI data were acquired, all data presented below were parcelled into four time windows. A 1 min time window that ended with ROC was flanked by two 2.5 min time windows, spaced with 2.5 min from the ROC time window, 'sedation' and 'post', respectively. An additional 2.5 min time window 'recovery' was defined at the end of the acquisition sequence. An additional temporal segmentation analysis was conducted, with varying ROC time windows of 2 and 2.5 min, and 'sedation' time windows of 1 and 3 min. In choosing these time windows, our aim was to balance between sufficient data time points and the dynamic nature of emergence which we sought to capture, while ruling out potential idiosyncrasies arising from a specific temporal windows selection.

Statistical analysis

First-level single study general linear models (GLMs) were prepared with the second sequence (fMRI Sequence 2, containing the moment of ROC). The conditions of interest were defined according to the subjects' state of consciousness, and periods between these conditions were defined as a confounder and marked as 'don't-care'. The GLM contained four conditions of interest: sedation, ROC, post-sedation, and recovery. The predictors were convolved with a standard haemodynamic response function (HRF). Movement regressors were included as confounders in the GLM to account for possible head movement related variance. To account for the long scan and sedated state, in addition to the standard motion correction, we applied spike information as noise related predictors. To evaluate the neural impact of the procedure, we conducted second-level whole brain random effect group analysis (RFX-GLM) (n=17 subjects). The centres of activation were identified with a significance threshold of P<0.02 (false discovery rate [FDR] corrected), with a minimal cluster size of 25 voxels. In order to examine whether patterns of activation obtained at the group level were similar to those obtained at the individual level, we randomly selected 10 subjects from the first level analysis and examined the compatibility of their activation pattern compared with the pattern obtained at the group level. The centres of activation were identified with a significance threshold of P<0.05 (not corrected).

Selection of ROIs

ROIs were selected from the preliminary neural activity analysis contrasting ROC *vs* sedation conditions. ROIs included the mammillary body (MB), median raphe (MR), RDLPT, thalamus and right inferior frontal gyrus (rIFG), chosen at a statistical threshold of P<0.02 (FDR corrected). The ventral tegmental area (VTA) and locus coeruleus (LC) were identified after relaxation of the statistical threshold to P<0.03 (FDR corrected). Using the Harvard Ascending Arousal Network (AAN) atlas[17] provided in the MNI space, and MNI2TAL conversions (Yale BioImage suite, New Haven, CT. USA), the coordinates of the ROIs were validated. Supplementary Table S1 provides the Talairach coordinates for the centres of the selected regions.

Functional connectivity analysis

A whole-brain psychological–physiological interaction (PPI)[18,19] random effect GLM analysis was conducted to test functional connectivity of the functionally identified ROIs. Regressors included the regressor of the specific experimental condition (psychological variable), the time course in a seed ROI (physiological variable) and the interaction between them. Subsequently, contrast images of the interaction gained from the PPI analyses were introduced to a random effects group (RFX-GLM) analysis and tested for statistical significance with a threshold of P<0.01 (uncorrected). Briefly, 1.5 mm sphere ROIs (19 voxels surrounding peak of activation) were functionally extracted from the contrast of 'ROC *vs* Recovery'. These clusters were extracted using the Brain Voyager plug-in: 'Talairach Coordinate to VOI' (Brain Innovation) and anatomically validated using BrainVoyager Brain Tutor Tool and neurosynth.org: (http://www.neurosynth.org/). In order to compare connectivity between the experimental conditions, beta values were generated for each VOI over all conditions (i.e. sedated, ROC, post-sedation, and recovery).

Results

The data shown in this study focus on emergence from deep sedation. This part of the experimental time line was parcelled into four time windows: sedation, ROC, post-sedation (tightly grouped, with 2.5 min between them), and a recovery time window at the end of the scans, summarised in Fig. 1a, with propofol concentrations for each time window shown in Fig. 1b. The average propofol concentration during ROC

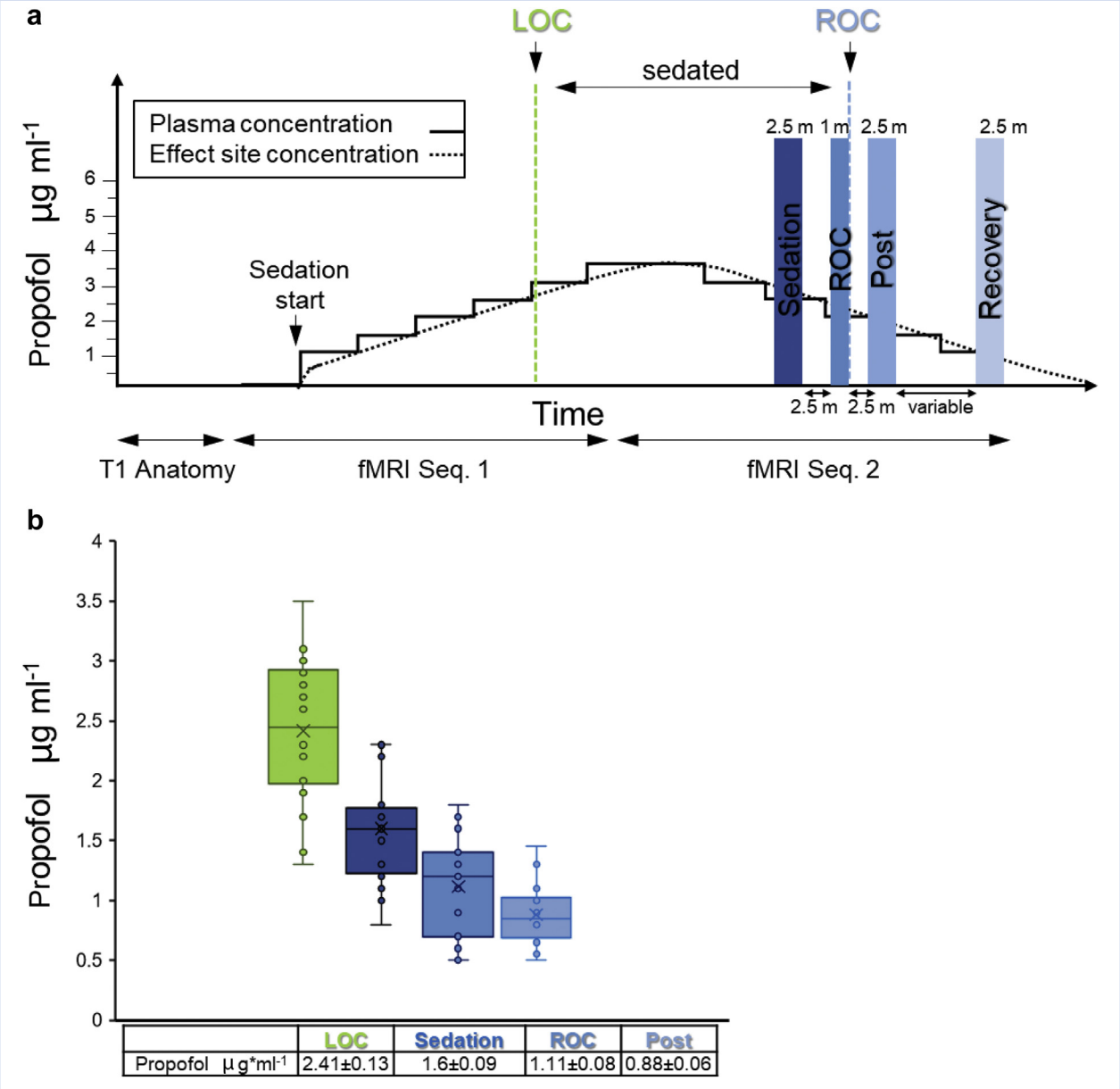

Fig 1. Experimental protocol. (a) Experimental timeline. After an anatomical sequence, the time line was parceled into four time windows: sedation, ROC, post-sedation, and recovery. Sedation procedure, using target-controlled infusion (TCI) of propofol, commenced. Starting with an effect site calculated concentration of 1 μg ml^{-1} with 0.5 μg ml^{-1} increments every 5 min. Sedation was titrated to loss of response to verbal stimulation—loss of consciousness (LOC). After a steady-state of deep sedation, serial decrements of propofol (0.5 μg ml^{-1} every 5 min) until return of consciousness (ROC) was verified as each participant responded to his name being called. It should be noted that each participant achieved LOC and ROC at different propofol concentrations, thus at different times throughout the session. Subsequent inter-subject analyses were made possible by alignment of the moment of emergence from sedation (ROC) between participants. As a result, the time from ROC to the recovery time window was variable. (b) Predicted propofol concentrations at various time windows. Propofol concentrations were derived from the pharmacokinetic calculator. Data in table are presented as mean (standard error of the mean). In the graph, x represents the mean, horizontal line the median.

was 50% lower than that during the LOC time window, and virtually identical to that in the post-sedation time window (2.41, 1.6, 1.11, and 0.88 μg ml^{-1}, respectively).

Neural activity during emergence from propofol deep sedation

Neural responses during different conditions were analysed using a GLM by contrasting different time windows. The contrast of 'Sedation' and 'ROC' conditions was selected to reflect brain activity during emergence. The analysis revealed multiple subcortical and cortical activations (Fig. 2, $P<0.02$, FDR corrected; see also Supplementary Fig. S1 for individual maps). Details for clusters of activity and their Talairach coordinates are provided in Table 1. Within the subcortical activations, we identified the MB, VTA, LC (right) and MR, components of the ARAS, and the thalamus. Additionally, we identified a pontine locus, unrelated to the ARAS, located in the RDLPT, which was found to affect the arousal state of patients with pontine lesions.[14]

In addition to subcortical activations, a wide set of cortical and cerebellar areas was found including right and left inferior temporal gyri, right superior frontal gyrus and left middle frontal gyrus, and posterior dorsal anterior cingulate cortex.

Functional connectivity analyses

As we found neural activations in discrete subcortical loci known to promote or be involved in the regulation of arousal, we performed functional connectivity analyses for these loci. To that end, we performed PPI analyses with specific ROIs. RDLPT, LC, MB, MR, VTA, and medial left thalamus were used as the seed ROIs (Fig. 3a–f, Table 2, Supplementary Table S1 and Fig. S2).

For all seed ROIs, most correlated regions were found to be subcortical—namely, the medulla was functionally correlated with the RDLPT; pontine loci were correlated with the RDLPT, MR, LC, and VTA. All the seed ROIs were correlated with the midbrain loci. Thalamic seeds were correlated to the midbrain. Lastly, the MR, VTA, LC, and thalamic seeds were also functionally correlated with the basal ganglia. Only a few cortical regions were functionally correlated with the seed ROIs: the RDLPT and MR had but one cortical functional connectivity (to the right medial temporal gyrus). The MB, VTA, and the thalamic seed, with multiple subcortical functional correlations, were functionally connected, within the cortex, to the insula only. The LC was correlated to the superior temporal and the inferior frontal gyri.

Next, we plotted beta values for the functional correlations of the resulting loci for all time windows (Fig. 4a–g, blue

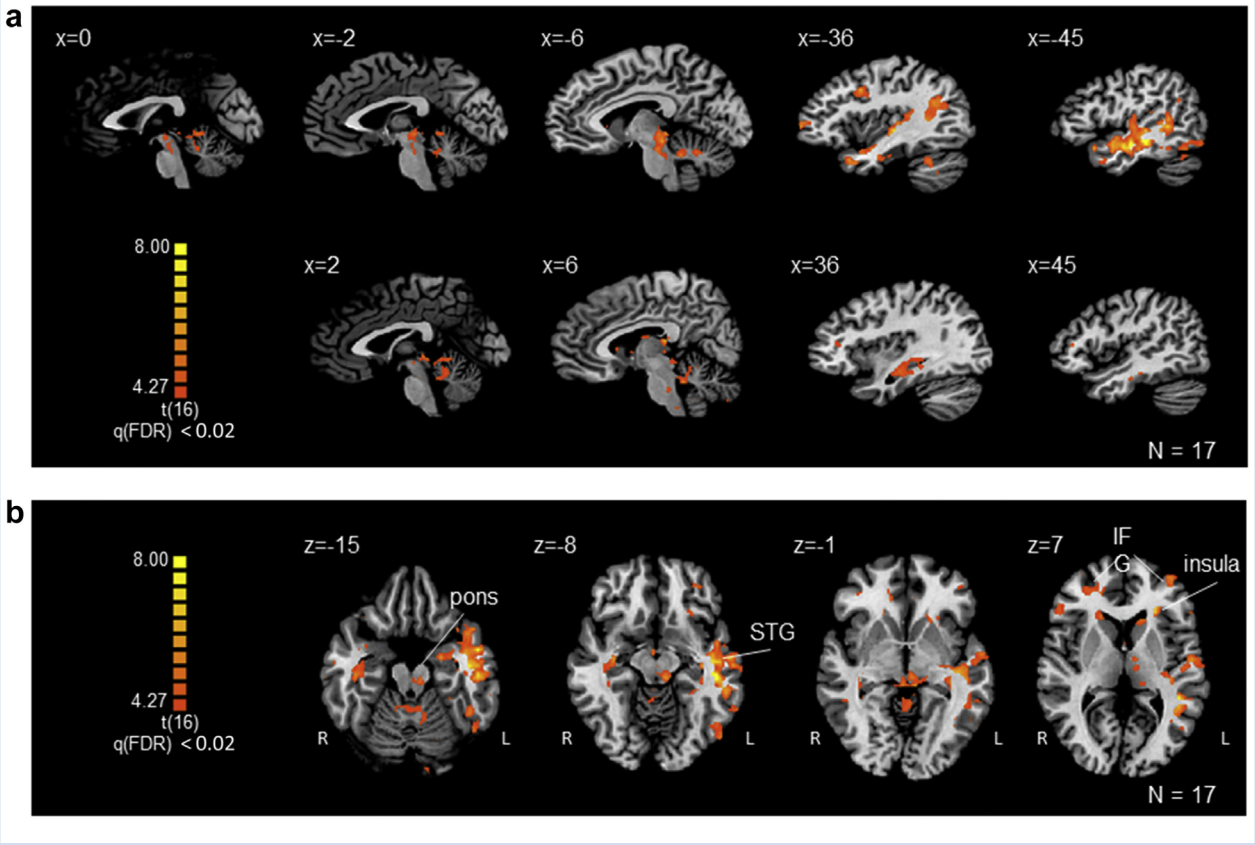

Fig 2. Neural activations upon emergence. Contrast of fMRI blood oxygen level dependent (BOLD) signals between the two time windows ROC *vs* Sedation are shown. (a) Sagittal sections. (b) Axial sections. Lateralisation of cortical signals, primarily temporal, can be seen. FDR, false discovery rate; fMRI, functional magnetic resonance imaging; STG, superior temporal gyrus.

Table 1 Activation network for ROC *vs* sedation contrast. Brain areas of significant activation during sequence II, practice Talairach coordinates. The activation centres were identified with the significance threshold set to $P<0.02$ (FDR corrected), with minimum cluster size set to 25 voxels. FDR, false discovery rate; IFG, inferior frontal gyrus; PAG, periaqueductal grey; pdACC, posterior dorsal anterior cingulate cortex; ROC, return of consciousness.

		X	Y	Z	*Cluster size*	t	P
Superior frontal gyrus	R	21	21	35	556	4.561	0.0003
Superior frontal gyrus	R	20	50	32	240	4.430	0.0004
Middle frontal gyrus	L	−20	40	25	304	4.548	0.0003
Middle frontal gyrus	L	−20	14	42	820	4.559	0.0003
IFG	R	43	33	9	279	4.939	0.0002
IFG	L	−33	4	32	1042	4.994	0.0002
pdACC	R	11	6	34	132	4.723	0.0002
pdACC	L	−8	1	35	233	4.642	0.0002
Superior-middle temporal gyrus	L	−45	−8	−12	3243	5.387	0.0001
Superior temporal gyrus	L	−45	−20	−3	2226	5.425	0.0001
Superior temporal gyrus	L	−38	11	−24	781	4.919	0.0002
Inferior temporal gyrus	R	54	−13	−21	394	4.839	0.0002
Parahippocampal gyrus	L	−24	−6	−16	423	4.840	0.0002
Caudate-head	L	−14	19	3	419	5.076	0.0001
Caudate-body	L	−12	11	14	66	4.444	0.0004
Caudate-body	R	8	15	6	81	4.490	0.0003
Caudate-head	R	17	24	3	209	5.560	0.0000
Thalamus-medial dorsal nucleus	L	−8	−16	6	51	4.468	0.0004
Thalamus-ventral lateral nucleus	L	−7	−10	5	82	4.602	0.0003
Thalamus-pulvinar	L	−13	−30	11	252	4.617	0.0003
Thalamus-pulvinar	R	8	−25	13	154	4.828	0.0002
Mammilary body	R	3	−9	−8	30	4.612	0.0003
Midbrain-PAG	L	−6	−27	−5	818	4.919	0.0002
Midbrain-pons	L	−6	−27	−17	367	4.642	0.0003
Medulla	BIL	3	−34	−41	62	4.608	0.0003
Cerebellum-culmen	L	−6	−44	−17	447	4.569	0.0003
Cerebellum	L	−8	−54	−17	416	4.548	0.0003
Cerebellum	L	−25	−38	−26	1941	4.927	0.0002
Cerebellum-Cerebellar lingual	R	4	−43	−15	559	4.481	0.0004

panels). The following recurring pattern emerged: functional correlations that were positive at the time of emergence turned negative at the next time window (post-sedation, 2.5 min after emergence), intensifying in the recovery time window.

To rule out the possibility that the emergent correlation patterns were arbitrary, we performed several control analyses. First, we tested additional loci in each PPI analysis. Specifically, (i) primary sensory areas such as primary auditory (A1+) and primary visual (V1+); (ii) areas involved in the executive functions, that is medial frontal and inferior frontal gyri; and (iii) the anterior and posterior cingulate gyri regions involved in the default mode network (DMN) which are implicated in the generation of 'internal awareness' and have previously been shown to be activated after emergence from sedation.[23] The patterns of positive correlations upon emergence and negative correlations thereafter were not observed in most of these instances (Fig. 4a–g, red panels).

Secondly, we performed PPI analysis using the rIFG (that was active in the same GLM contrast, in which all other ROIs were selected) as the seed ROI (Figs 3g and 4g). The resulting beta correlations demonstrated a different pattern, one of gradual increase, from negative correlations during sedation to positive correlations upon recovery.

Third, we performed a temporal analysis with slight variation in time window selection in order to rule out the possibility that results were idiosyncratic to the selected time windows, thus impairing their generalisability. The activation patterns in the tested ROIs were very similar to those obtained in the original analysis (Supplementary Fig. S3).

Discussion

We performed a two-step analysis by selecting significant neural activations during emergence from deep sedation in a data-driven approach as seed ROIs for subsequent functional connectivity analysis. We found a functional connectivity spatio-temporal sequence that accompanies, and possibly drives, emergence from deep sedation. Its two distinctive features are: (1) subcortical predominance of loci correlated with the seeds and (2) a pattern of transient positive correlations upon emergence that abruptly turn to negative correlations thereafter.

Localisation of ARAS components

The ARAS, a collection of nuclei that promotes wakefulness and participates in the regulation of physiological sleep,[9,11,20,21] has been implicated in the effects of hypnotic drugs on consciousness. Identification of discrete subcortical loci should be approached with caution, but identification of the aforementioned loci has been reported.[17,18,22–25] In our neural activation analysis, we identified multiple components of the ARAS: primarily the dopaminergic VTA, noradrenergic LC, histaminergic MB, and serotonergic MR. Of these ARAS components, only the VTA was found to be functionally connected to the thalamus during emergence from sedation.

Cortical activations during emergence

At emergence from sedation, multiple cortical activation loci were observed. As the stimulus for emergence was calling a

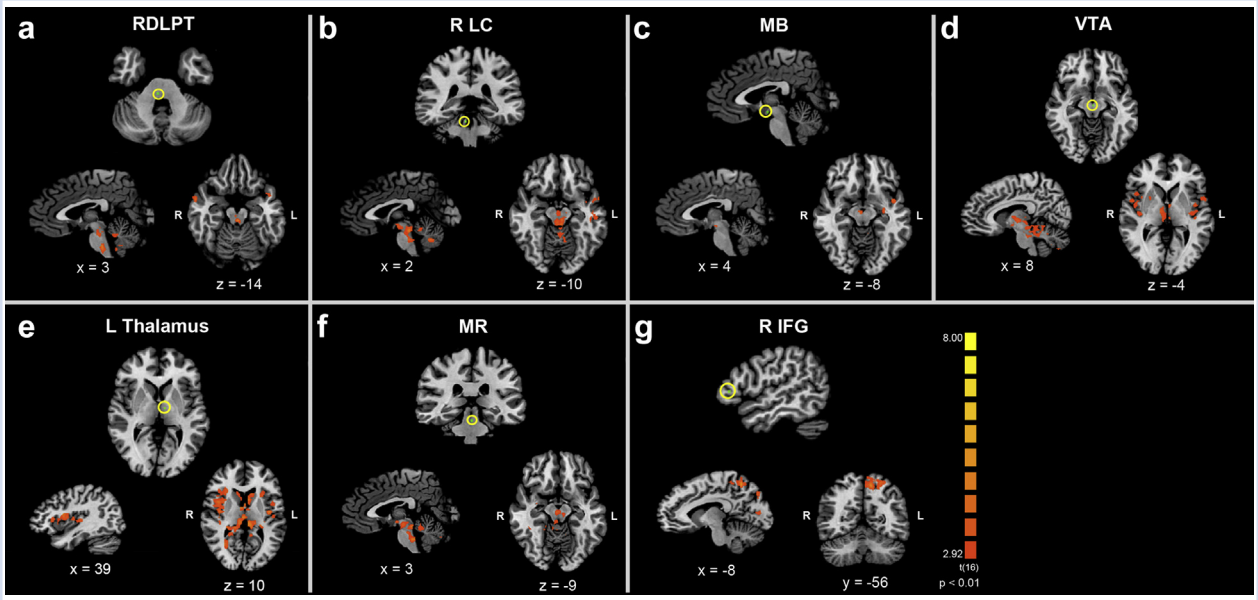

Fig 3. Psychophysiological interaction (PPI) analyses. Functional connectivity was assessed using PPI. Seed regions of interest (ROIs) are marked with yellow circles. Resulting views for each PPI analysis, within Talairach space, are shown for (a) rostral dorsolateral pontine tegmentum (RDLPT), (b) locus coeruleus (LC), (c) mammillary body (MB), (d) ventral tegmental area (VTA), (e) left medial thalamus seed, (f) median raphe (MR), and (g) right inferior frontal gyrus (rIFG) as a control to the subcortical seed ROIs. $P<0.01$ without false discovery rate (FDR) correction.

participant's name, observed activation in the left superior temporal gyrus may reflect processing of linguistic stimuli and not directly related to emergence. Other cortical activity patterns were scarce, and primarily frontal. PPI analysis was conducted in the rIFG as a control ROI for the subcortical seeds. This showed a spatiotemporal sequence of a gradual increase of functional connectivity, distinct from the predominant subcortical sequence.

The observed relative paucity of cortical activations is in agreement with Langsjo and colleagues[2] and Xie and colleagues.[3] Our data differ from these studies in the fact that we did not observe activations associated with the DMN: the posterior cingulate cortex (in both studies) and the anterior cingulate cortex (in the Langsjo and colleagues study). A possible explanation for this discrepancy is our ability to resolve the moment of emergence as a discrete event, whereas the other studies contrasted sedation with recovery time windows without capturing the actual moment of emergence.

Evidence supporting active emergence from sedation

We propose the interpretation of the observed functional connectivity spatiotemporal sequence as evidence for active reanimation, that is emergence from sedation as an active process. This is in contrast to exogenous administration of drugs to facilitate emergence, that is methylphenidate,[4] orexin receptor agonist,[6] or physostigmine,[3] but rather endogenous neural activity: the transient increased functional connectivity of multiple subcortical loci may not only accompany, but also drive emergence. There are multiple arousal promoting loci with possible redundancy.[26] Our results imply a convergent effect of multiple arousal promoting loci during emergence from sedation. After emergence, we found negative correlations of arousal promoting loci. This should not be interpreted as if no arousal promoting signals are needed to maintain arousal, but may highlight the redundancy of arousal promoting pathways that may be active but segregated (hence anti-correlated). Were emergence a passive process, determined mainly by the reduction in concentrations of hypnotic agents,[7] one would expect a different functional connectivity spatiotemporal sequence, such as that of the rIFG, which showed a pattern of gradual increase in connectivity from sedation to recovery, concomitant with alterations in propofol levels.

A cautious attempt to connect these facts to the pre-existing theoretical background of consciousness studies yields a similarity to Laurey and colleagues'[27] description of wakefulness and awareness as two dimensions of consciousness. The subcortical functional connectivity sequence of arousal-promoting loci represents increased wakefulness. Awareness, or the content of consciousness, may be represented by the rIFG used as a seed ROI for the executive network which showed a different profile with a more gradual increase in functional connectivity from sedation to recovery. Such a gradual increase in functional connectivity of cortical seed regions is in accordance with the integrated information theory.[28]

RDLPT, coma, and emergence

Fischer and colleagues[14] recently described a pontine locus that is strongly associated with coma-causing lesions. We identified a pontine locus that resides within the aforementioned locus, although the peak coordinate reported here is different. This locus exhibits a similar functional connectivity pattern to known ARAS components during emergence. The

Table 2 Psychophysiological interactions (PPI) networks. Brain areas of significant correlation with seed region, practice Talairach coordinates. 1.5 mm sphere ROIs (19 voxels-surrounding peak of correlation) were functionally extracted from the correlation maps with the contrast of ROC *vs* Recovery. The brain regions were identified with the significance threshold set to $P<0.01$ (uncorrected). IFG, inferior frontal gyrus; PAG, periaqueductal grey; ROC, return of consciousness; STG, superior temporal gyrus; VTA, ventral tegmental area.

PPI-rostral dorsolateral pontine tegmentum (RDLPT)							
Parahippocampal gyrus	R	24	4	−29	178	3.46	0.004
Midbrain-PAG	BIL	0	−28	−14	71	3.52	0.004
Pons-midbrain tegmentum	BIL	2	−23	−17	114	3.24	0.005
Midbrain	BIL	1	−22	−10	28	3.11	0.006
Pons	L	−5	−28	−33	60	3.18	0.006
Pons	R	3	−28	−34	211	3.47	0.004
Medulla	BIL	1	−28	−40	104	3.3	0.005
Cerebellum	L	−4	−52	−32	262	3.23	0.005
PPI-locus coeruleus (LC)							
IFG	R	30	34	−11	57	3.32	0.005
STG	L	−51	4	−9	195	3.44	0.004
STG	R	56	4	−13	101	3.34	0.004
Caudate	R	17	7	13	89	3.35	0.005
Putamen	L	−22	9	5	196	3.15	0.006
Midbrain-PAG	BIL	0	−27	−12	1173	3.4	0.004
VTA	BIL	1	−15	−7	315	3.31	0.005
Pons-RDLPT	BIL	−2	−32	−25	499	3.64	0.003
Pons	L	−7	−29	−20	186	3.4	0.004
Cerebellum	BIL	1	−57	−26	427	3.42	0.004
Cerebellum	BIL	−2	−42	−16	554	3.23	0.005
PPI-mammillary bodies (MB)							
Insula	L	−40	0	−7	125	3.35	0.004
Midbrain-VTA	R	4	−14	−8	40	3.36	0.004
Midbrain	L	−8	−19	−10	71	2.85	0.012
PPI-ventral tegmental area (VTA)							
Insula	R	39	5	7	56	2.7	0.016
Putamen	R	20	6	−3	218	2.8	0.0127
Striatum	R	25	−5	−4	458	2.91	0.011
Striatum	L	−26	−10	−4	277	2.83	0.012
Thalamus	R	8	−12	4	315	2.94	0.0107
Midbrain-tegmentum	L	−4	−23	−13	521	3.16	0.008
Hypothalamus	R	3	−4	−7	129	2.85	0.012
Pons	R	2	−26	−18	355	2.89	0.011
Cerebellum	L	−20	−56	−19	312	2.8	0.013
Cerebellum	R	30	−56	−22	387	2.87	0.016
Cerebellum	R	13	−20	−40	567	3.004	0.0092
PPI thalamus							
Insula	R	39	1	11	2044	3.37	0.004
Posterior insula	L	−38	−12	7	1260	3.59	0.003
Median thalamus	BIL	1	−20	8	421	3.65	0.003
Pulvinar	R	8	−25	10	516	3.85	0.002
Pulvinar	L	−9	−28	10	716	3.77	0.002
Hippocampus	R	25	−35	7	428	3.96	0.002
Caudate	L	−7	9	7	954	3.41	0.004
Caudate	R	7	13	8	188	3.16	0.006
Midbrain	L	−2	−26	−9	206	3.29	0.005
Midbrain	R	9	−29	−10	158	3.24	0.005
PPI-median raphe nucleus (MR)							
Parahippocampal gyrus	R	28	−3	−18	338	3.114	0.007
Uncus	R	33	−3	−32	314	3.241	0.005
Uncus	L	−27	5	−30	221	3.243	0.005
Middle temporal gyrus	L	−44	3	−21	332	3.421	0.004
Putamen	L	−21	1	3	184	3.3	0.005
Midbrain-VTA	BIL	2	−20	−9	351	3.3	0.005
Midbrain	BIL	3	−29	−12	319	3.308	0.005
Midbrain-thalamic junction	BIL	2	−11	−4	220	3.25	0.005
Pons-midbrain	L	−5	−33	−17	565	3.214	0.005
Pons	BIL	2	−32	−29	654	3.361	0.005
Cerebellum (culmen)	L	−25	−49	−24	748	3.302	0.005
Cerebellum (lingual)	BIL	2	−41	−14	559	3.108	0.007
Cerebellum (pyramis)	L	−10	−71	−26	321	3.089	0.007
Cerebellum (uvula)	R	17	−73	−25	272	3.1	0.007
PPI-right inferior frontal gyrus (RIFG)							
Superior frontal gyrus	L	−3	−20	47	342	3.48	0.003
Superior frontal gyrus	R	1	−20	47	208	3.59	0.003
Post central gyrus	R	42	−20	54	1625	3.5	0.003
Pre/post central gyrus	L	−36	−23	51	2461	3.55	0.003
Precuneus	L	−13	−57	53	3302	3.37	0.005
Precuneus	L	−17	−77	38	1809	3.27	0.005

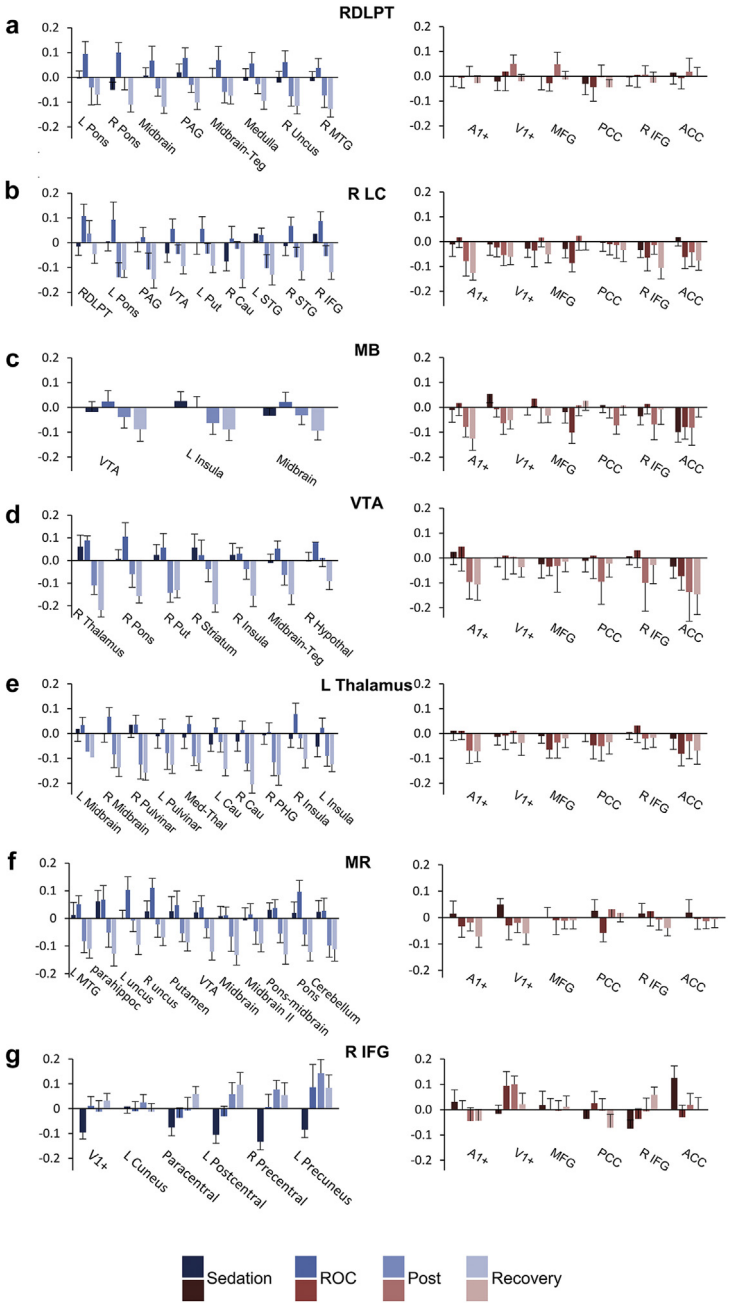

Fig 4. Functional connectivity profiles. For each seed ROI, functionally connected loci are shown (blue panels). Beta values (covariate values between the seed and each locus) for all analysed time windows: sedation, ROC, post-sedation and recovery. Red panels represent control loci, related to sensory pathways, executive networks and the DMN (selected from the literature). (a–f) Subcortical seed ROIs selected functionally from the neural activations contrast ROC *vs* Sedation. An emerging correlation pattern emerged in which peak correlation were found in the ROC time window followed by negative correlations in subsequent time windows (blue panels). Mostly negative correlations, without a signature pattern, were found in internal controls (red panels). (g) Right inferior frontal gyrus (rIFG) cortical activation seed ROI. A pattern of increasing correlations, from negative correlations in the sedated time window to positive correlations in the post-sedation and recovery time windows, is distinct from the subcortical correlations pattern (a–r). RDLPT, rostral dorsolateral pontine tegmentum; LC, locus coeruleus; MB, mammillary body; MR, median raphe; VTA, ventral tegmental area; PAG, periaqueductal grey; Teg, tegmentum; Put, putamen; Cau, caudate; IFG, inferior frontal gyrus; MTG, medial temporal gyrus; STG, superior temporal gyrus; PHG, parahippocampal gyrus; MFG medial frontal gyrus. PCC, posterior cingulate cortex; ACC, anterior cingulate cortex; A1+, primary auditory cortex; V1+, primary visual cortex; ROC, return of consciousness; ROI, region of interest.

finding of a locus that plays a part both in coma and in emergence from deep sedation points to an association between these states.

Limitations and future studies

Although our analytic time windows were tightly packed and marked an advance in temporal resolution, they may still be regarded as a compromise. Future studies should include dynamic resting state fMRI in order to further increase the temporal resolution of emergence from sedation. Our study focused specifically on emergence. Although we related results to the dual dimensions of consciousness proposed by Laurey and colleagues,[27] our data for the networks that represent awareness, consciousness' content dimension, were scarce and derived originally as a cortical control to the subcortical seeds. Future studies may directly investigate distinctive patterns of functional connectivity in wakefulness and awareness by expanding the networks representing the content of consciousness. In order to be able to relate to subcortical ROIs, we were forced to relax some of our thresholds for secondary analysis (PPI of subcortical loci) up to $P<0.01$ (uncorrected). Although such practice has been successful,[14] lack of statistical stringency increases the likelihood of a false positive signal.

Authors' contributions

Research design: TN, AOB, TH, IM.
Research: TN, AOB, EI, YL.
Data analysis: AOB, YL, TN.
Drafting of the manuscript: AOB, YL, TN.
All authors approved the final version of the manuscript.

Declarations of interest

The authors declare that they have no conflicts of interest.

Funding

Internal institutional research funding of the TASMC and Department of Anaesthesiology, Pain and Critical Care of the TASMC. Israeli Society of Anaesthesiologists grant (TN).

Acknowledgements

We thank the following people: Anat Cattan for help with regulatory coordination; Alexander Sutman and Daniel Stocki for help with sedation procedures, Dafna Ben Bashat and Moran Artzi for help with planning of the acquisition sequences, Joshua Mincer and Vicky Myers for their thoughtful advice and critical reading of the manuscript.

Appendix A. Supplementary data

Supplementary data to this article can be found online at https://doi.org/10.1016/j.bja.2019.05.038.

References

1. Purdon PL, Pierce ET, Mukamel E, et al. Electroencephalogram signatures of loss and recovery of consciousness from propofol. *Proc Natl Acad Sci U S A* 2013; **110**: E1142–51
2. Langsjo JW, Alkire MT, Kaskinoro K, et al. Returning from oblivion: imaging the neural core of consciousness. *J Neurosci* 2012; **32**: 4935–43
3. Xie G, Deschamps A, Backman SB, et al. Critical involvement of the thalamus and precuneus during restoration of consciousness with physostigmine in humans during propofol anaesthesia: a positron emission tomography study. *Br J Anaesth* 2011; **106**: 548–57
4. Solt K, Cotten JF, Cimenser A, Wong KFK, Chemali JJ, Brown EN. Methylphenidate actively induces emergence from general anesthesia. *Anesthesiology* 2011; **115**: 791–803
5. Larijani GE, Goldberg ME, Hojat M, Khaleghi B, Dunn JB, Marr AT. Modafinil improves recovery after general anesthesia. *Anesth Analg* 2004; **98**: 976–81
6. Kelz MB, Sun Y, Chen J, et al. An essential role for orexins in emergence from general anesthesia. *Proc Natl Acad Sci U S A* 2008; **105**: 1309–14
7. Brown EN, Lydic R, Schiff ND. General anesthesia, sleep, and coma. *N Engl J Med* 2010; **363**: 2638–50
8. Alkire MT, Hudetz AG, Tononi G. Consciousness and anesthesia. *Science* 2008; **322**: 876–80
9. Jones BE. Arousal systems. *Front Biosci* 2003; **8**: s438–51
10. Lydic R, Baghdoyan HA. Sleep, anesthesiology, and the neurobiology of arousal state control. *Anesthesiology* 2005; **103**: 1268–95
11. Franks NP, Zecharia AY. Sleep and general anesthesia. *Can J Anesth* 2011; **58**: 139–48
12. Taylor NE, Solt K. Optogenetic activation of dopamine neurons in the ventral tegmental area induces reanimation from general anesthesia. *Proc Natl Acad Sci* 2016; **113**: 12826–31
13. Parvizi J, Damasio A. Neuroanatomical correlates of brainstem coma. *Brain* 2003; **126**: 1524–36
14. Fischer DB, Boes AD, Demertzi A, et al. A human brain network derived from coma-causing brainstem lesions. *Neurology* 2016; **87**: 2427–34
15. Ramsay MAE, Savege TM, Simpson BRJ, Goodwin R. Controlled sedation with alphaxalone–alphadolone. *BMJ* 1974; **2**: 656–9
16. Talairach J, Tournoux P. Co-planar stereotaxic atlas of the human brain: 3-dimensional proportional system: an approach to cerebral imaging. *Neuropsychologia* 1988; **39**: 145
17. Edlow BL, Takahashi E, Wu O, et al. Neuroanatomic connectivity of the human ascending arousal system critical to consciousness and its disorders. *J Neuropathol Exp Neurol* 2012; **71**: 531–46
18. O'Reilly JX, Woolrich MW, Behrens TEJ, Smith SM, Johansen-Berg H. Tools of the trade: psychophysiological interactions and functional connectivity. *Soc Cogn Affect Neurosci* 2012; **7**: 604–9
19. Raz G, Jacob Y, Gonen T, et al. Cry for her or cry with her: context-dependent dissociation of two modes of cinematic empathy reflected in network cohesion dynamics. *Soc Cogn Affect Neurosci* 2014; **9**: 30–8
20. Nelson LE, Guo TZ, Lu J, Saper CB, Franks NP, Mazel M. The sedative component of anesthesia is mediated by $GABA_A$ receptors in an endogenous sleep pathway. *Nat Neurosci* 2002; **5**: 979–84
21. Saper CB, Chou TC, Scammell TE. The sleep switch: hypothalamic control of sleep and wakefulness. *Trends Neurosci* 2001; **24**: 726–31
22. Zhang J-T, Ma S-S, Yip SW, et al. Decreased functional connectivity between ventral tegmental area and nucleus accumbens in Internet gaming disorder: evidence from

resting state functional magnetic resonance imaging. *Behav Brain Funct* 2015; **11**: 37
23. Kang P, Lee J, Sul S, Kim H. Dorsomedial prefrontal cortex activity predicts the accuracy in estimating others' preferences. *Front Hum Neurosci* 2013; **7**: 1–11
24. Minzenberg MJ, Watrous AJ, Yoon JH, Ursu S, Carter CS. Modafinil shifts human locus coeruleus to low-tonic, high-phasic activity during functional MRI. *Science* 2008; **322**: 1700–2
25. D'Ardenne K, McClure S, Cohen JD. D'ardenne. BOLD responses reflecting dopaminergic signals in the human ventral tegmental area. *Science* 2013; **339**: 816–9
26. Edlow BL, Takahashi E, Wu O, et al. Neuroanatomic connectivity of the human ascending arousal system critical to consciousness and its disorders. *J Neuropathol Exp Neurol* 2012; **71**: 531–46
27. Laureys S, Boly M, Moonen G, Maquet P. Two dimensions of consciousness: arousal and awareness. *Neuroscience* 2009; **2**: 1133–42
28. Tononi G. An information integration theory of consciousness. *BMC Neurosci* 2004; **5**: 42

Handling editor: H.C. Hemmings Jr